Published OnlineFirst December 11, 2014; DOI: 10.1158/1078-0432.CCR-14-0492

Cancer Therapy: Preclinical

Clinical Cancer Research

CD99 Triggering in Ewing Sarcoma Delivers a Lethal Signal through p53 Pathway Reactivation and Cooperates with Doxorubicin

Clara Guerzoni[1,2], Valentina Fiori[3], Mario Terracciano[1], Maria Cristina Manara[1,2], Diego Moricoli[3], Michela Pasello[1,2], Marika Sciandra[1], Giordano Nicoletti[2], Mara Gellini[4], Sabrina Dominici[5], Claudia Chiodoni[6], Pier Maria Fornasari[7], Pier-Luigi Lollini[8], Mario P. Colombo[6], Piero Picci[1,2], Maurizio Cianfriglia[4], Mauro Magnani[3,5], and Katia Scotlandi[1,2]

Abstract

Purpose: The paucity of new drugs for the treatment of Ewing sarcoma (EWS) limits the cure of these patients. CD99 has a strong membranous expression in EWS cells and, being also necessary for tumor survival, is a suitable target to aim at. In this article, we described a novel human monospecific bivalent single-chain fragment variable diabody (dAbd C7) directed against CD99 of potential clinical application.

Experimental Design: *In vitro* and *in vivo* evaluation of cell death and of the molecular mechanisms triggered by anti-CD99 agents were performed alone or in combination with doxorubicin to demonstrate efficacy and selectivity of the new dAbd C7.

Results: The dAbd C7 induced rapid and massive EWS cell death through Mdm2 degradation and p53 reactivation. Mdm2 overexpression as well as silencing of p53 in p53wt EWS cells decreased CD99-induced EWS cell death, whereas treatment with nutlin-3 enhanced it. Furthermore, cell death was associated with induction of p21, bax, and mitochondrial depolarization together with substantial inhibition of tumor cell proliferation. Combined treatment of anti-CD99 dAbd C7 with doxorubicin was additive both *in vitro* and *in vivo* against EWS xenografts. Normal mesenchymal stem cells showed no p53 activation and were resistant to cell death, unless transformed by EWS-FLI, the oncogenic driver of EWS.

Conclusions: These results indicate that dAbd C7 is a suitable candidate tool to target CD99 in patients with EWS able to spare normal stem cells from death as it needs an aberrant genetic context for the efficient delivery of CD99-triggered cell death. *Clin Cancer Res; 21(1); 146–56. ©2014 AACR.*

Introduction

Ewing sarcoma (EWS) is a relatively rare mesenchymal tumor that hits preferentially children and adolescents. Roughly 70% of patients with localized disease at diagnosis can now be cured with conventional agents (1) at risk of suffering low quality of life due to limb-salvage procedures, prolonged dose-dense chemotherapy, development of chronic severe pathologies and risk of secondary malignancies (2). For patients with metastasis prognosis remains grim (3) and few treatments can be offered to those who relapse after first-line therapies. Rarity of the disease has limited substantial advances in therapy and any improvements mainly rely on public investments. Therefore, development of suitable drugs in academia may represent a first step to develop new therapeutics for EWS and, in this effort, anti-CD99 approaches are very promising (4, 5).

Although present on the X chromosome, the *MIC2* gene encoding for CD99 does not undergo X inactivation (6). The crucial biologic processes involving CD99 include lymphocyte development, cell adhesion and monocyte diapedesis, and expression of TCR, MHC class I and II as well as of some adhesion molecules (i.e., ELAM-1, VCAM-1, ICAM-1) by mobilization of these molecules from the Golgi to the plasma membrane (7–14). In pathology, CD99 is found on the cell surface of EWS, acute lymphoblastic leukemia, thymic tumors, some spindle cell tumors (e.g., synovial sarcoma), hemangiopericytoma, meningioma, and malignant glioma, in which it confers high invasiveness and low survival rates (13, 15–18). In EWS, the EWS-FLI1 oncogenic activity (19) is facilitated by CD99 likely because it hampers cell differentiation maintaining an high proliferation rate (20). Indeed CD99 knockdown in EWS cells induces terminal neural differentiation and reduces

[1]CRS Development of Biomolecular Therapies, Experimental Oncology Laboratory, Istituto Ortopedico Rizzoli, Bologna, Italy. [2]PROMETEO Laboratory, STB, RIT Department, Istituto Ortopedico Rizzoli, Bologna, Italy. [3]DIATHEVA s.r.l., Fano, Italy. [4]Department of Medicine Research and Evaluation, Italian National Institute of Health, Rome, Italy. [5]Deparment of Biomolecular Sciences, Section of Biochemistry and Molecular Biology University of Urbino "Carlo Bo," Urbino, Italy. [6]Molecular Immunology Unit, Department of Experimental Oncology and Molecular Medicine, Fondazione IRCCS "Istituto Nazionale dei Tumori," Milan, Italy. [7]PROMETEO Laboratory, RIT Department, Istituto Ortopedico Rizzoli, Bologna, Italy. [8]Department of Experimental, Diagnostic and Specialty Medicine, Laboratory of Immunology and Biology of Metastasis, Bologna, Italy.

Note: Supplementary data for this article are available at Clinical Cancer Research Online (http://clincancerres.aacrjournals.org/).

Corresponding Authors: Katia Scotlandi, Rizzoli Orthopaedic Institute, via di barbiano, 1/10, Bologna 40136, Italy. Phone: +39 051 6366760; Fax: +39 051 6366763; E-mail: katia.scotlandi@ior.it; and Mauro Magnani. Phone: +39 0722 305211; E-mail: mauro.magnani@uniurb.it

doi: 10.1158/1078-0432.CCR-14-0492

Published OnlineFirst December 11, 2014; DOI: 10.1158/1078-0432.CCR-14-0492

Translational Relevance

We presented a new therapeutic agent in the format of human monospecific diabody (dAbd C7) against CD99 to be exploited in the treatment of Ewing sarcoma, a pediatric tumor with still unmet therapeutic needs. dAbd C7 was able to efficiently deliver a cell death message inside an oncogene-driven cellular context but not in normal cells. Acting through Mdm2 degradation and p53 reactivation, the diabody is likely to be effective in the great majority of Ewing sarcoma thanks to the rarity of p53 mutations in this tumor and effectively combined with doxorubicin, potentially opening up a new avenue for therapeutic intervention in these patients.

tumor growth and bone metastasis upon transplantation into immunodeficient mice (20). In turn, EWS-FLI1 maintains high levels of CD99 expression (20–23). Triggering CD99 with selected mouse antibodies induces cell death in leukemic and EWS cells (4, 24, 25) and inhibits EWS growth and metastasis formation (5). Therefore, CD99 is a suitable target for EWS also considering that it is easily accessible, is expressed in virtually all cases (15) and it has a role in the pathogenesis of this tumor.

To translate this information into a possible clinical application, we felt necessary to document the selective delivery of death signals to EWS cells while sparing normal cells and to develop a nonimmunogenic human recombinant antibody against CD99. In particular, we developed a recombinant monospecific diabody (named dAbd C7) from the human single-chain fragment variable (scFv) antibody backbone (26), exploiting the fact that diabodies are bivalent antigen-binding molecules with higher affinity and stability compared with scFvs, although being small and easily manipulated (27). We demonstrated that CD99 triggering induces Mdm2 ubiquitination and degradation, which leads to p53 reactivation. Accordingly, engagement of CD99 by dAbd C7 significantly increases efficacy of doxorubicin *in vitro* and *in vivo*. We also showed that ligation of CD99 by antibodies does not affect viability or differentiation of normal human mesenchymal stem cells (h-MSC) expressing high levels of the molecule and that delivery of a death message is favored by the presence of the EWS-FLI oncogene, the genetic hallmark of EWS.

Materials and Methods

Cell lines and primary cell cultures

EWS cell lines have been authenticated by STR PCR analysis; detailed information in Supplementary Methods. Stable transfection was performed with: pCMV or pCMV-MDM2 to overexpress MDM2; pCDNA3.1-Flag-p53 human to obtain forced expression of p53 by using Calcium Phosphate Transfection Kit (Invitrogen). Transient silencing was performed with: Validated STEALTH siRNA (Invitrogen) for p53, EF-22 (5′-GUACGGGCAGCAGAGUUCUU-3′) for EWS-FLI1 type II (Ambion), EWS-FLI1 (5′-GCAGAACCCUUCUUAUGACUU-3′) and EWS-FLI2 (5′-GGCAGCAGAACCCUUCUUAUU-3′) for EWS-FLI1 type I (Ambion) by using Lipofectamine 2000 (Invitrogen). Cells were cultured in Iscove's modified Dulbecco's medium (IMDM; Gibco), supplemented with 100 U/mL penicillin, 100 μg/mL streptomycin, and 10% inactivated FBS (Lonza) or IMDM with neomycin (Sigma, 500 μg/mL).

Murine C3H10T1/2 transfected with EWS-FLI1 (C3H10T1/2 EF) and h-MSCs were obtained and cultured as previously described (28). All cell lines have been tested for mycoplasma contamination (Mycoplasma detection Set, Takara Bio Inc.) before use.

Anti-CD99 treatments

Treatments with the anti-CD99 0662-mAb were performed as previously described (4, 25). Treatments with dAbd C7, obtained from scFv C7 (26) by shortening the linker length between the VH and VL of scFv C7 from 15 to 5 residues, were performed according to the same guidelines at the concentration of 200 μg/mL where not differently specified. Annexin V–propidium iodide (PI) staining was evaluated with Mebcyto apoptosis Kit (MBL); mitochondrial depolarization was analyzed with JC-1 (5,5′,6,6′-tetrachloro-1,1′,3,3′ tetraethylbenzimidazolylcarbocyanine iodide) staining (Molecular Probes). For proteasome or p53/Mdm2-interaction inhibition assays, cells were treated, respectively, with MG132 (10 μmol/L; Calbiochem) for 3 hours, or with nutlin-3 (5 μmol/L) for 24 hours before 0662-mAb. 6647 EWS cell line was treated simultaneously with dAbd C7 at 200 μg/mL and escalating doses of doxorubicin from 1 ng/mL to 30 ng/mL. After 72 hours of treatment, the effect of the combination was evaluated by MTT assay kit (Roche Diagnostics GmbH). Combination index (CI) was calculated with the isobologram equation (29) by using the CalcuSyn software (Biosoft).

Microarray, antibody array, and bioinformatic analysis

6647 cells treated with anti-CD99 0662-mAb were profiled for gene expression by using 1A (V2) Oligo Microarray G4110B slides (Agilent Technologies) and for proteomic analysis by the Kinex antibody microarray (KAM-1.1). For a complete description, see Supplementary Materials and Methods. Microarray data are available at GEO with accession number GSE36097. Gene/protein alterations were functionally analyzed with Ingenuity (Ingenuity Systems, Inc.; www.ingenuity.com) or GeneGo (GeneGo Inc.; www.genego.com) softwares; output data were filtered for P value less than 0.05.

Western blotting and immunoprecipitation

Cells were lysed with phospho-protein extraction Buffer (Upstate) supplemented with protease-phosphatase cocktail inhibitor (Sigma). Proteins of interest were detected with specific antibodies; for a detailed list, see Supplementary Materials and Methods. For immunoprecipitation, 500 μg of cell lysates were incubated for 16 hours with Protein G-Plus agarose beads (Calbiochem) in the presence of 1 μg anti-Mdm2 or control IgG antibody (Calbiochem). Immunoprecipitates and 50 μg total lysates were then resolved on a 10% Tris-HCl gel and immunoblotted with specific antibodies.

RNA extraction and quantitative real-time PCR

RNA extraction and quantitative real-time PCR (qPCR) of anti-CD99–treated cells were performed as previously described (20). Primers sequences are available in Supplementary Materials and Methods.

In vivo treatments with dAbd C7 alone or in combination with doxorubicin

Female athymic 4- to 5-week-old Crl:CD-1nu/nuBR mice (Charles River Italia) were subcutaneously injected with

Published OnlineFirst December 11, 2014; DOI: 10.1158/1078-0432.CCR-14-0492

5×10^6 6647 cells. The animals were randomized into five groups: in the group treated with dAbd C7 alone, each mouse received subcutaneous injections of dAbd C7 (1 mg/injection) for each day for two subsequent cycles of five days. The second group received doxorubicin intraperitoneal injection (50 μg/injection) on the seventh and the eighth days after cell seeding injection (5). The third group received 10 subcutaneous injections of dAbd C7 (1 mg/injection) and intraperitoneal injection of doxorubicin (50 μg/injection) with the same schedule of single treatment. Control mice received subcutaneous injections of PBS (same volume/injection; 10 injections) or vehicle. Tumor growth and body weight was assessed once a week by measuring tumor volume, calculated as $\pi/2\ [\sqrt{(a\ b)}]^3/6$ where a and b are the two maximum diameters. For ethical reasons, mice with local tumors were killed when they achieved a tumor volume of 3 mL and necropsied. Before the sacrifice, blood samples and spleens were collected from all the experimental groups and processed to assess specific parameters, for a detailed description see Supplementary Materials and Methods. Experimental protocols were reviewed and approved by the Institutional Animal Care and Use Committee ("Comitato Etico Scientifico per la Sperimentazione Animale") of the University of Bologna, and forwarded to the Italian Ministry of Health with letter 4783-X/10 (responsible researcher Prof. C. De Giovanni).

Immunohistochemical analysis

Avidin–biotin–peroxidase procedure was used for immunostaining of formalin-fixed, paraffin-embedded tumors xenografts. Detection of Ki-67 was performed after pretreatment with a citrate buffer solution with MIB-1 antibody (1:100 dilution; Calbiochem-Novabiochem). TUNEL assay and anti-CD99 were performed with ApopTag Plus Peroxidase *In Situ* Apoptosis Kit (Merck Millipore) according to manufacturer's instructions, and with O13 monoclonal antibody (1:80 dilution; Covance), respectively.

Statistical analysis

Differences among means were analyzed using Student t test; χ^2 test was used for frequency; the CI of multiple treatments was calculated with the isobologram equation with CalcuSyn software (Biosoft) to identify synergistic/additive/antagonistic effects.

Results

CD99 triggering reactivates p53 through Mdm2 degradation

We analyzed a panel of 14 EWS patient-derived cell lines testing their susceptibility to death induced by the mouse anti-human CD99 0662-mAb and found that after 30-minute exposure 9 cell lines were very sensitive (the percentages of alive cells after CD99 triggering was significantly different: 7 cell lines; **, $P < 0.001$, 2 cell lines $P < 0.05$, Student t test), whereas the remaining five were rather resistant (not significant differences; Supplementary Table S1). To gain information on which transcriptional death pattern might be activated, the most susceptible cell line 6647 was analyzed for both global gene expression (30 minutes–2 hours) and phospho-proteins (5 minutes–1 hour) following 0662-mAb exposure. Gene expression profile identified 366 differentially expressed mRNAs (Fisher test significant difference for a 5% error; Supplementary Table S2), suggesting that CD99-dependent cell death is an active process requiring transcriptional modulation. Moreover, significant posttranslational modifications ($\geq$2 fold change) were identified in 71 of 600 proteins as early as 5 minutes after exposure to 0662-mAb (Supplementary Table S3). Annotation analysis of RNA microarray and antibody array profiling identified changes involving ERK/MAPK pathway, mitochondrial dysfunction, and apoptosis signaling (Fig. 1A). Network analysis highlighted involvement of p53 (Fig. 1B) and accordingly, increase of bax and the cell-cycle inhibitor CDKN1A (p21), two well-known transcriptional targets of p53 (30), together with bcl-2 decrease were confirmed by Western blotting upon 0662-mAb treatment (Fig. 1C). Consistently, 0662-mAb cell death was triggered with different efficacy depending on the p53 status (Fig. 1D). Cell lines carrying wild-type (wt) p53 or carrying minor P53 alterations conserving some transcriptional activity, were killed more effectively than cell lines displaying truncations, major deletions or mutations inactivating P53 transcription that appeared to be more resistant to anti-CD99 treatment (31, 32). The 6647 cell line, carrying the single point mutation S241F in the DNA-binding domain, retains only part of wt-p53 activity, as confirmed by reporter assays (Supplementary Table S4), and behaves like the RD-ES cell line that carries the R273C point mutation (33).

Sensitive EWS cell lines, namely 6647, LAP-35, and WE-68, were specifically phosphorylated at p53 ser-15 after treatment with the 0662-mAb (Fig. 2A, Supplementary Fig. S1A), but not at other phospho-specific sites (Supplementary Fig. S1B). In contrast, the p53-truncated TC-71 cell line, which is more resistant to anti-CD99 treatment (Fig. 1D), did not show sign of p53 stabilization nor phosphorylation (Fig. 2A). mRNA levels of *Gadd45-α*, a gene transcriptionally induced by p53, were also markedly increased in sensitive cells after CD99 triggering (Fig. 2B). To test whether p53 activation is a step necessary for CD99-induced cell death, p53 was silenced in 6647 and LAP-35 cells and, conversely, forcely expressed in p53-deficient EWS cells (Fig. 2C and Supplementary Fig. S1C). Silencing of p53 significantly reduced, while forced expression of wt-p53 enhanced 0662-mAb–induced cell death, in comparison with scramble siRNA or empty vector–transfected cells (Fig. 2C and Supplementary Fig. S1C).

In EWS, p53 is rarely mutated while preferentially inactivated by Mdm2 (34), an E3 ubiquitin ligase that antagonizes the p53 tumor suppressor by inhibiting its ability to transactivate target genes or by promoting its degradation/nuclear export (35). Accordingly, triggering of CD99 markedly and rapidly (15 minutes) downmodulated Mdm2 in LAP-35 and, in a dose-dependent manner, in 6647 cells (Fig. 3A). Such downmodulation was due to polyubiquitination and proteasome-dependent degradation of Mdm2 that followed CD99 engagement as shown by immunoprecipitation and Western blot analysis as well as by its rescue using the proteasome inhibitor MG132 (Fig. 3B). Likewise, pretreatment of LAP-35 and 6647 cells with MG132 markedly decreased the percentage of cell death induced by 0662-mAb treatment (Fig. 3B), suggesting that reduced Mdm2 expression/activity favors cell death. To further assess the role of Mdm2/p53 signaling in CD99-induced cell death, we generated LAP-35 cells stably expressing Mdm2 (LAP-35-MDM2) or carrying the pCMV empty vector (LAP-35-EV) and tested their susceptibility to death upon treatment with 0662-mAb. LAP-35 cells ectopically expressing Mdm2 showed

Published OnlineFirst December 11, 2014; DOI: 10.1158/1078-0432.CCR-14-0492

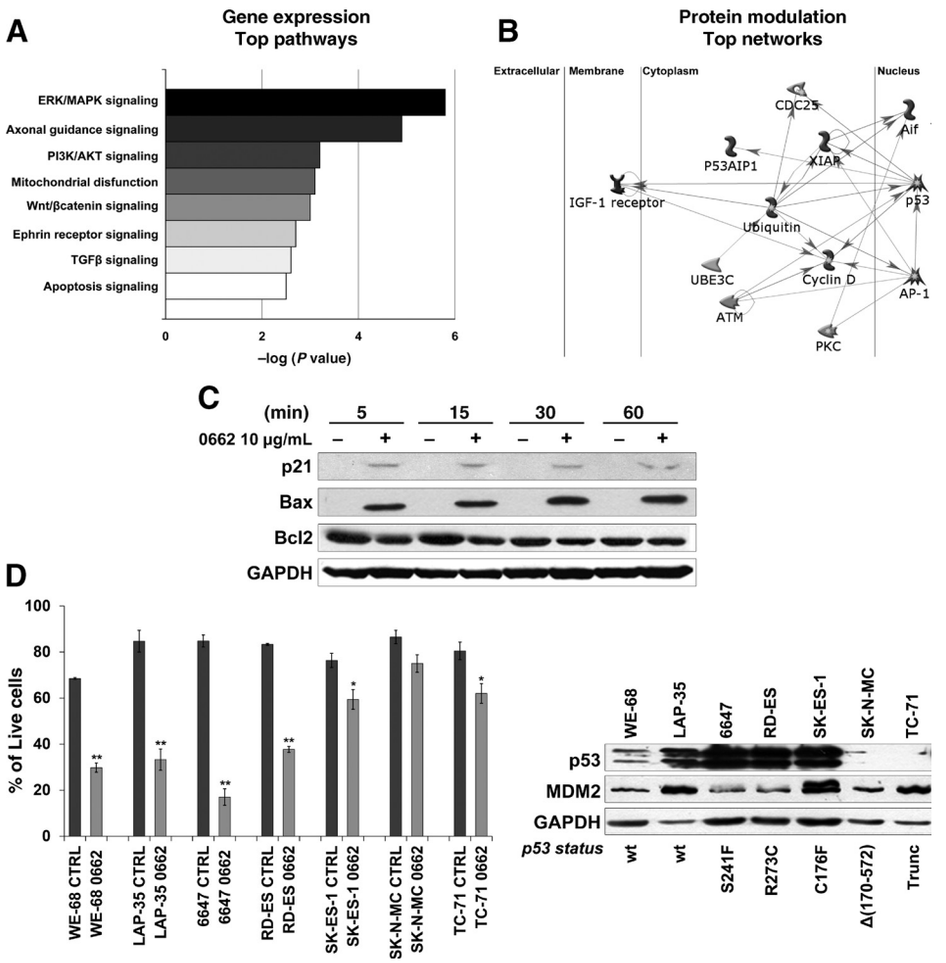

Figure 1.
CD99 targeting induces changes in gene expression and posttranslational modifications in EWS cells. A, annotation analysis of gene expression modulations ($P < 0.05$) in 0662-mAb–treated 6647 EWS cells according to Ingenuity software. B, GeneGo analysis of protein modulations after mAb treatment highlights a p53 converging network. C, Western blot analysis of Bax, Bcl-2, and p21 on untreated (−) and 0662-mAb–treated (+) 6647 cells. Equal loading was monitored by anti-GAPDH blotting. D, left, annexin V–PI analysis in EWS cell lines before and after 30-minute treatment with 10 μg/mL 0662-mAb. Values are expressed as mean of at least three independent experiments of live cells (**, $P \leq 0.001$ Student t test for WE-68, LAP-35, 6647 and RD-ES; *, $P < 0.05$ for SKES-1 and TC-71). Right, Western blot analysis of p53 and Mdm2 protein levels in EWS cell lines; p53 genetic status is described. Equal loading was monitored by anti-GAPDH blotting.

lower levels of p53 and partial reversion from cell death than LAP-35-EV in response to 0662-mAb treatment (Fig. 3C). Combined treatment with 0662-mAb and nutlin-3, an inhibitor of the p53–Mdm2 interaction (36), markedly reduced percentage of live cells in comparison with treatment with the sole antibody (Fig. 3D). Effects of nutlin-3 were also confirmed by evaluating the mitochondrial membrane potential of LAP-35 cells treated with 0662-mAb. After JC-1 staining, mitochondrial depolarization occurred upon CD99 engagement; mitochondrial membrane potential collapse increases in nutlin-3–pretreated LAP-35 cells (Fig. 3D). These findings indicate that CD99 triggering reactivates p53 via Mdm2 degradation by ubiquitination. Considering that degradation of p53 by Mdm2 is the prevalent mechanism of p53 inactivation in EWS, CD99 triggering may induce cell death in the great majority of patients with EWS.

EWS-FLI1 favors the delivery of the CD99-induced cell death message

Although broadly expressed at low levels in several normal cell types, high expression of CD99 occurs in few cellular context, mainly Sertoli and immune cells (7, 37). In normal lymphocytes, CD99-induced cell death correlates with their maturation stage being more effective in immature lymphocytes (38, 39). However, hematopoietic CD34-positive cells and h-MSCs, which express high levels of CD99 (40), are resistant to anti-CD99 mAb (5, 41). Indeed, seven primary cultures of h-MSC derived from bone marrow, dental pulp, and corion, all displaying CD99 at levels similar to those of EWS cells, did not show any sign of significant death when exposed to 0662-mAb treatment (Fig. 4A). Accordingly, cells displayed nonphosphorylated p53 (Fig. 4A), no induction in p53 downstream genes like *GADD45α* (Supplementary Fig. S2A), while maintaining the ability to differentiate towards osteoblasts (Supplementary Fig. S2B).

We thus tested whether the CD99-induced cell death requires the oncogenetic cellular context driven by EWS-FLI1 to explain the differences with normal cell counterpart. To this end, the murine C3H10T1/2 mesenchymal cells transfected with both EWS-FLI1 and CD99 (20) were treated with 0662-mAb. These cells underwent cell death and phosphorylation of serine 15 of p53 within 1 hour (Fig. 4B). Accordingly, silencing of EWS-FLI1 in LAP-35 cells reduced CD99-induced cell death, without affecting CD99 expression levels (Fig. 4C). Overall, these findings suggest that anti-CD99 mAbs deliver a massive cell death message preferentially in an aberrant cellular context, thus

Published OnlineFirst December 11, 2014; DOI: 10.1158/1078-0432.CCR-14-0492

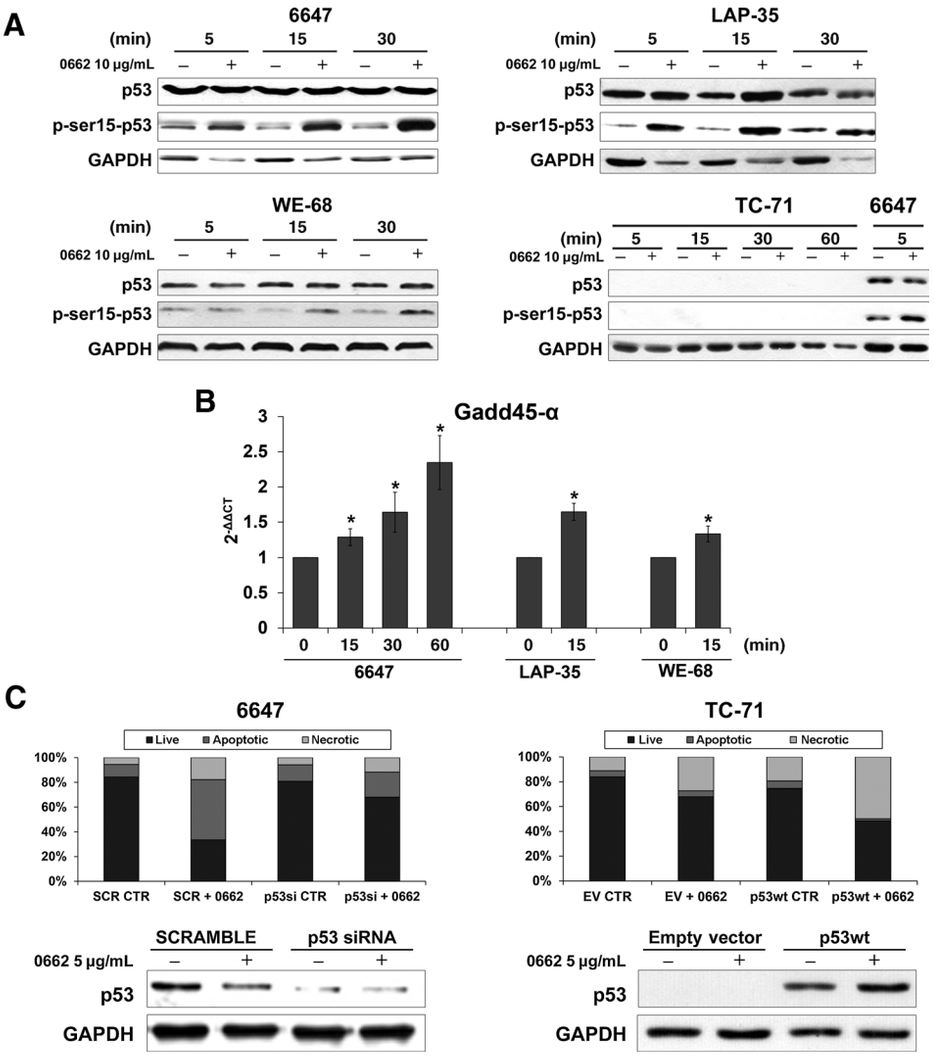

Figure 2.
0662-mAb induces ser-15 p53 phosphorylation. A, Western blot analysis of total and ser-15–phosporylated p53 on whole cell lysates from untreated (−) or treated (+) 6647, LAP-35, WE-68, and TC-71 EWS cells. B, histogram shows qPCR evaluation of Gadd45-α mRNA after 10 μg/mL 0662-mAb treatment (mean ± SE, two experiments with three replicates/each). GAPDH expression was used as internal control (*, $P < 0.05$, Student t test). C, annexin V–PI analysis in EWS cells after silencing (6647 p53si) or forced expression of p53 (TC-71 p53wt) after treatment (30 minutes) with 0662-mAb. Values are from one experiment representative of two ($P < 0.001$ for 6647; $P < 0.05$ for TC-71, X^2 test with respect to scramble or empty vector–transfected cells). Bottom, Western blot analysis of p53 levels in corresponding cells before and after treatment. Equal loading was monitored by anti-GAPDH blotting.

supporting a sufficient level of specificity for possible clinical translation.

Development of human anti-CD99 C7 diabody

The above results obtained using a murine antibody prompted us to develop a suitable reagent for clinical use. We engineered the scFvs C7 directed against CD99 (26) to develop a bivalent antigen-binding molecule (dAbd C7) characterized by a doubled valency and a molecular mass of about 55–60 kDa to reduce the too fast clearance typical of monomers and increase tumor retention (42, 43). ELISA and Annexin V-PI assays demonstrated the higher avidity and activity of dAbd C7 over scFv C7, respectively (Supplementary Fig. S3).

Although the kinetics was partly different compared with the murine 0662-mAb, the dAbd C7 induced the death of EWS cells (Fig. 5A). TC-71 and SK-N-MC cells, with deleted or truncated p53, were still the most resistant cell lines, confirming the involvement of p53. Accordingly, dAbd C7 induced Mdm2 inhibition and ser15-p53 phosphorylation in 6647 EWS cells but not in h-MSC cells (Fig. 5B) where dAbd C7 was ineffective (Supplementary Fig. S4A). In addition, similarly to the murine 0662-mAb, dAbd C7 was able to reactivate p53 (Fig. 5C) in C3H10T1/2 EFCD99 leading to cell death (Supplementary Fig. S4B). To further demonstrate that the p53 pathway is critical also for the cytotoxic action of the dAbd C7, p53 was silenced in 6647 and LAP-35 cells and, conversely forcely expressed in p53-deficient EWS cells demonstrating reversion or enhancement of the dAbd C7 efficacy (Fig. 5D and Supplementary Fig. S4C).

Combination with doxorubicin increases dAbd C7 therapeutic activity

Considering the ability of reactivating the functional p53 signaling, CD99 ligation by dAbd C7 qualifies for combination with conventional agents such as doxorubicin, which is a leader drug in the management of EWS. Combination of dAbd C7 with doxorubicin produced additive effect (CI: 0.820 ± 0.238) *in vitro* (Supplementary Fig. S5A) and *in vivo*, reduced significantly the growth of 6647 tumor xenografts (mean values of tumor volumes in controls vs. dAbd C7+ doxorubicin-treated mice: CTR 1.47 ± 0.29 vs. 0.49 ± 0.16, $P = 0.03$;

Published OnlineFirst December 11, 2014; DOI: 10.1158/1078-0432.CCR-14-0492

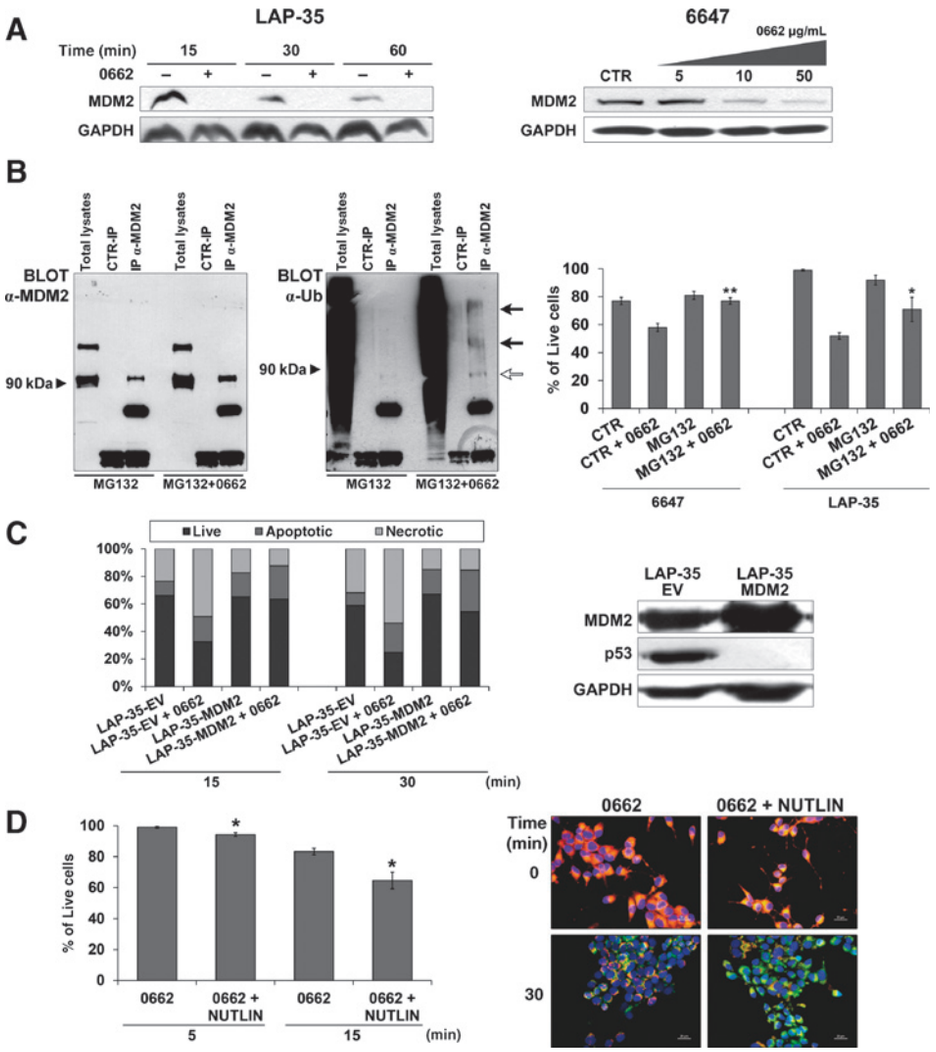

Figure 3.

Mdm2 protein levels decrease upon 0662-mAb treatment. A, left, time-dependent modulation of Mdm2 expression in LAP-35 cells after treatment with 0662-mAb (10 μg/mL) by Western blot analysis. Right, dose-dependent modulation of Mdm2 in 6647 cells after 15-minute treatment with 0662-mAb (5–50 μg/mL). B, left, Western blot evaluation of Mdm2 and ubiquitin on total cell lysates, anti-Mdm2, or anti-IgG immunoprecipitates from LAP-35 cells treated with MG132 alone or plus 0662-mAb. The empty arrow indicates Mdm2 unconjugated protein, the black arrows indicate ubiquitinated forms of Mdm2. Right, histogram depicting 6647 and LAP-35 percentage of viable cells (vital cell counting) before and after 16-hour treatment with 10 μg/mL 0662-mAb, alone or in combination with MG132. Data are shown as mean of at least two independent experiments ± SE; **, $P < 0.01$; *, $P < 0.05$; Student t test. C, left, annexin V–PI analysis in LAP-35-EV or LAP-35–MDM2 expressing cells, before and after treatment with 0662-mAb. Values are from one experiment representative of two ($P < 0.001$, with respect to empty vector-transfected cells, χ^2 test). Right, Western blots of Mdm2 and p53 protein levels in corresponding cells. Equal loading was monitored by anti-GAPDH blotting. D, left, histogram shows percentage of live cells assessed by annexin V–PI in LAP-35. Values are shown as mean of two independent experiments ± SE ($P < 0.05$; Student t test after 15 minutes). Right, JC-1 mitochondrial staining in adherent LAP-35 cells treated with 0662-mAb in presence or absence of nutlin-3. When mitochondrial membrane potential collapses, JC-1 cannot accumulate within mitochondria and remains in the cytoplasm in a green fluorescent monomeric form.

vehicle 1.51 ± 0.05 vs. 0.49 ± 0.16, $P < 0.001$, Student t test) in contrast to doxorubicin or dAbd C7 given as single agent (Fig. 6B). Tumors treated with the combination were completely avoided of proliferating cells (Ki-67 negative) while rich in TUNEL-positive cells (Fig. 6B, Supplementary Fig. S5B). Conversely, doxorubicin alone induced a certain degree of necrosis with large tumor areas that remained vital and highly proliferating. Treatment with dAbd C7 alone was able to abrogate tumor proliferation and induced cell death in half of the tumors, while in the less responsive ones appeared heterogeneous with areas of active proliferation besides areas showing signs of antibody efficacy. Notably, CD99 expression disappeared in tumors that were efficiently inhibited by dAbd C7.

A possible bystander effect of anti-CD99 approaches is the induction of the HSP70 that may activate NK cells cytotoxicity contributing to tumor elimination (44). To verify any possible involvement of this pathway in the efficacy of anti-CD99 therapy, we have assessed whether CD99 ligation induced HSP70

Published OnlineFirst December 11, 2014; DOI: 10.1158/1078-0432.CCR-14-0492

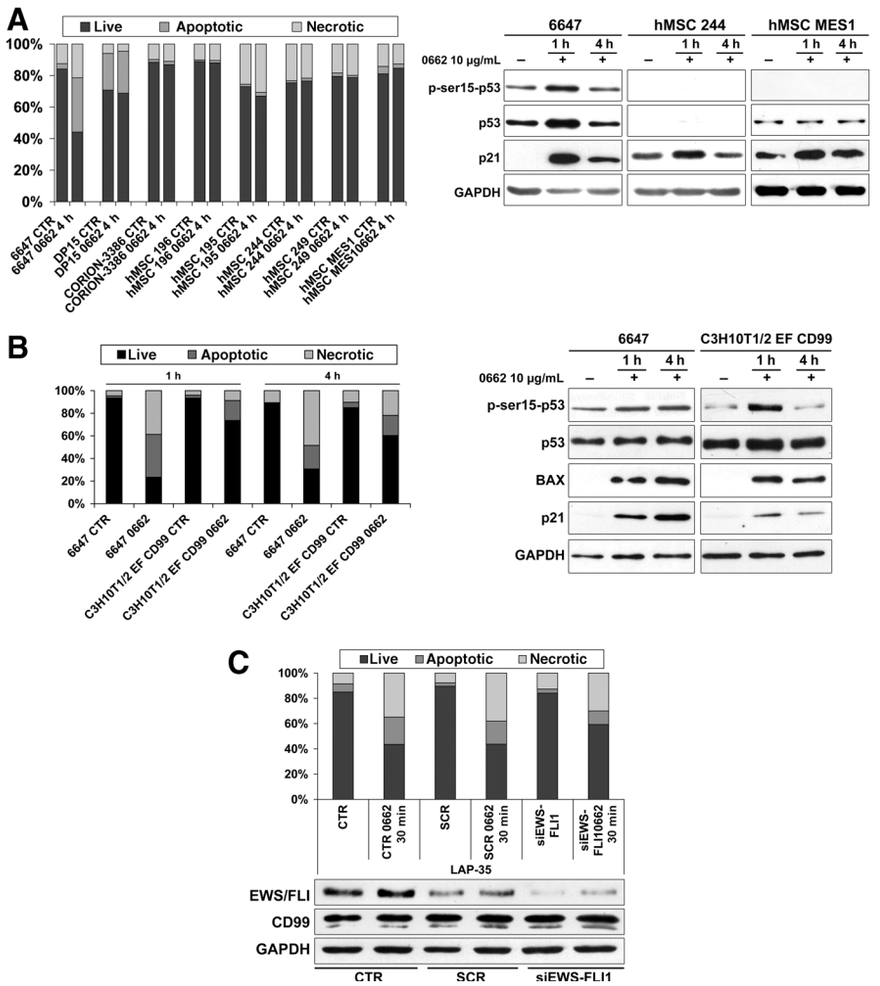

Figure 4.
Anti-CD99 0662-mAb does not affect mesenchymal stem cells. A, left, annexin V–PI positivity upon 0662-mAb treatment in 6647 or h-MSCs from different origins (dental pulp, DP15; corion, CORION-3386; bone marrow, h-MSCs). Data from one experiment representative of two. Right, Western blotting analysis of p21, ser-15-phosphorylated p53, and total p53 after treatment with 10 µg/mL 0662-mAb in the same cells. Equal loading was monitored by anti-GAPDH blotting. B, left, annexin V–PI evaluation of murine MSC C3H10T1/2 EF CD99 after treatment with 0662-mAb. Data from one experiment representative of two ($P < 0.001$, χ^2 test). Right, Western blotting analysis of p21, BAX, ser-15–phosphorylated p53, and total p53 after treatment with 10 µg/mL 0662-mAb in the same cells. Equal loading was monitored by anti-GAPDH blotting. C, annexin V–PI evaluation of control, scramble, or EWS-FLI1 silenced LAP-35 cells after treatment with 0662-mAb. Data from one experiment representative of two ($P < 0.05$ with respect to control or scrambled cells treated with 0662-mAb, χ^2 test). Western blots showed EWS-FLI1 silencing and CD99 expression in the same cells. Equal loading was monitored by anti-GAPDH blotting.

expression in EWS cells and analyzed the number and phenotype of NK cells in dAbd C7-treated nude mice xenotransplanted with EWS tumors. Differently from what observed in acute lymphoblastic leukemia (44), CD99 ligation did not induce HSP70 expression in EWS cells or in xenografts (Supplementary Fig. S6). Accordingly, the analysis of NK phenotype and activity in dAbd C7-treated nude mice xenotransplanted with EWS tumors did not show differences from untreated mice (Supplementary Table S5). Specifically, we have not observed any significant change in NK cells number (as NK1.1+ cells), activation/maturation state (CD69 and CD11b expression) and effector functions *in vitro* (as CD107a expression and production of IFNg), suggesting that NK cells are not involved in the efficacy of dAbd C7-based therapy. Considering that dAbd C7 was able to recognize the murine form of CD99 (not shown), treated mice were checked for weight, blood glucose and urea levels, hepatic enzymes and general signs of collateral toxicity. No changes were observed (Supplementary Table S6).

Discussion

CD99 has been proposed as an effective target to treat EWS because it promotes cancer cell death when triggered by specific antibodies (4). However, therapeutic tools of mouse origin find limited clinical exploitations due to rapid induction of patients human-anti-mouse-antibody responses, which severely reduce antibody effectiveness after few applications. Therefore, isolation and engineering of human whole antibodies or fragments represents the unique choice for a repeated use. Monoclonal antibodies in the format of scFvs are the smallest stable fragment of an antibody still able to bind to the antigen. They combine the advantage of a fully human sequence to that of small size, which allows better tumor penetration compared with full-length mAbs and production in large quantities by recombinant technology in bacterial systems without the need of animal immunization (42). In addition, scFvs can be modified in their size, pharmacokinetics, immunogenicity, specificity, valency, and effector functions to improve affinity and stability and reduce the rapid blood clearance (45). In this article, we engeneered the scFvs C7 directed against the CD99 molecule (26) to develop a monospecific bivalent antigen-binding molecule (dAbd C7) that was able to ligate efficiently CD99 and deliver a cell death message inside EWS cells. Molecular mechanisms activated by dAbd C7 were similar to those observed using the mouse monoclonal antibody 0662: both induced Mdm2 degradation

Published OnlineFirst December 11, 2014; DOI: 10.1158/1078-0432.CCR-14-0492

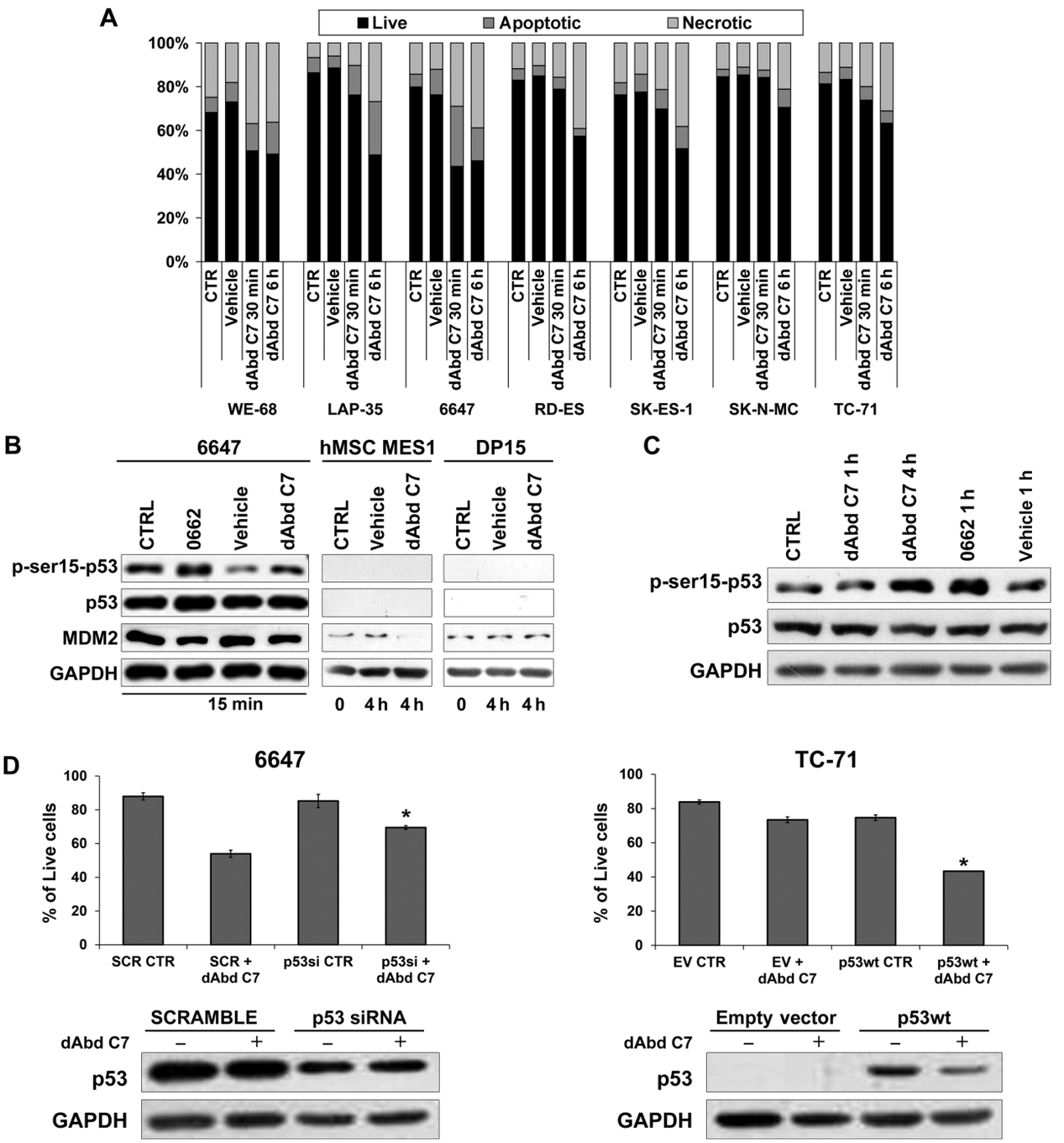

Figure 5.
Effects of the human single-chain diabody dAbd C7 against CD99 on EWS and MSC. A, annexin V–PI evaluation upon dAbd C7 200 μg/mL treatment in a panel of EWS cell lines after 30 minutes or 6 hours. B, Western blot of ser-15–phosphorylated p53, total p53 and Mdm2 after treatment with dAbd C7 (200 μg/mL), 0662-mAb (10 μg/mL), or vehicle alone in 6647 and two different h-MSCs. Equal loading was monitored by anti-GAPDH blotting. C, Western blot of ser-15–phosphorylated p53, total p53, and Mdm2 levels after treatment with 0662-mAb, dAbd C7 or vehicle alone in murine MSC C3H10T1/2 EF CD99. Equal loading was monitored by anti-GAPDH blotting. D, annexin V–PI analysis in EWS cells after silencing (6647p53si) or forced expression (TC-71p53wt) of p53 after treatment (30 minutes) with dAbd C7 200 μg/mL. Percentage of live cells are shown as mean of two independent experiments (*, $P < 0.05$ Student t test).

and lead to the tumor suppressor protein p53 reactivation. Considering that p53 is rarely mutated in EWS (less than 10%), but rather it is functionally inactivated by several mechanisms including overexpression of Mdm2 (31, 34, 46), anti-CD99 dAbd C7 may be potentially effective in the great majority of the cases. Moreover, due to its reactivating

Published OnlineFirst December 11, 2014; DOI: 10.1158/1078-0432.CCR-14-0492

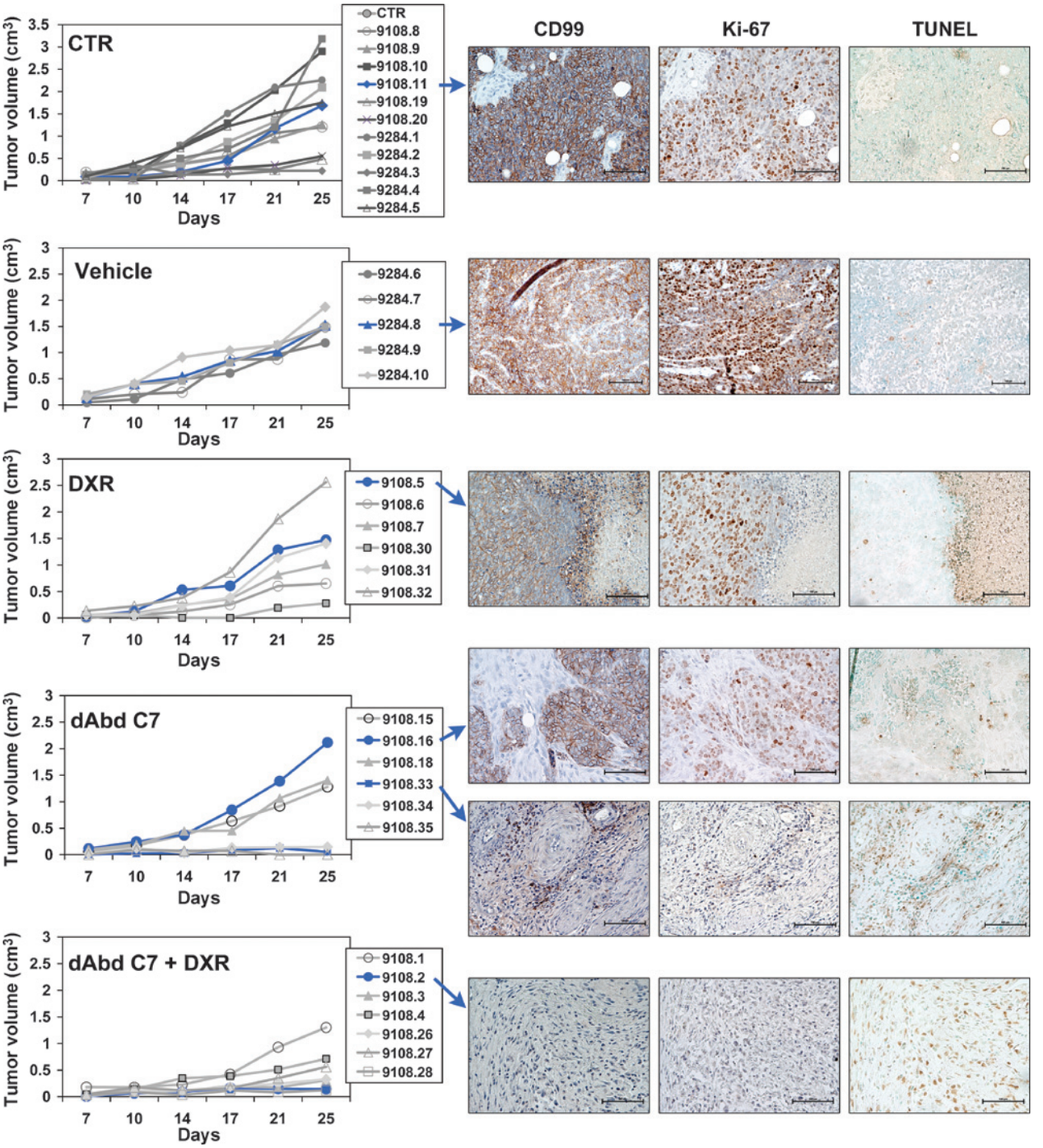

Figure 6.
Efficacy of dAbd C7 alone or in association with doxorubicin against 6647 xenografts. Tumor growth in the differently treated mice. Representative (corresponding to blue curve mice) immunohistochemical evaluation of CD99, Ki-67, and apoptotic nuclei in untreated or treated tumors (scale bar 100 μm) are shown. Mean tumor volumes at day 25 (when treatments stopped) indicated significant differences between controls and mice treated with dAbd C7 + doxorubicin (see results).

functions on p53 signaling, CD99 ligation by dAbd C7 qualifies for a potentially effective combination with conventional agents like doxorubicin, which besides binding to DNA-associated enzymes and intercalating with DNA base pairs, influences apoptosis pathways affecting bcl-2/bax, and/or AMP-activated protein kinase (AMPK) molecular signaling (47). By delivering complementary messages that converge on cell death, anti-CD99 dAbd C7 can thus potentiate the cytotoxic

effects of doxorubicin, a leader drug in the treatment of patients with EWS. Indeed, combined treatments gave additive antitumor effects *in vitro* and induced significant advantages in slowing tumor growth *in vivo*, in keeping with what observed with the murine 0662-mAb (5).

Before proposing clinical application of anti-CD99 dAbd C7, we felt also necessary to document the selective delivery of death signals to EWS cells. CD99 is broadly expressed in many normal cells at low levels with some notable exceptions, including immature T and B lymphocytes (11, 48). Although it was demonstrated that the cells expressing high levels of CD99 were more sensitive to CD99 antibody ligation than low expressing ones (4, 38), some effects on normal B lymphopoiesis were observed (38). However, total cell numbers decreased significantly below control upon CD99 ligation only after long-term incubations (7 days), a condition that very unlikely will be achieved *in vivo*, particularly with antibody fragments such as diabodies that have a rapid clearance from circulation (the terminal half-life of these molecules in mice is in the range of 5–6 hours; ref. 49). In addition, we showed here that induction of CD99-induced cell death also needs adjustment for genetic background. We found that both normal hematopoietic (5) and mesenchymal stem cells, which express very high levels of CD99 (41) did not die nor modify their differentiative potential when CD99 was engaged by the mouse 0662-mAb or the human dAbd C7. Consistently, we detected no activation of p53 in these normal cells, nor induction of downstream targets, with the only exception of p21, a protein that may be regulated also by p53-independent mechanisms (50). In contrast, when normal mesenchymal stem cells were transfected with EWS-FLI1, their susceptibility to CD99 ligation increased and p53 was reactivated. Similarly, c/pre-B leukemia blasts carrying the TEL/AML1 chimera were found to be more sensitive to CD99-induced cell death (44). These findings indicate that rapid and massive CD99-induced cell death may occur preferentially in an aberrant genetic background, when cells being forced to grow by oncogenetic stimuli could not recover stressful signals through cell-cycle exit and result more vulnerable, thus offering new fuel to support the therapeutic use of anti-CD99 dAbd C7 against EWS cells.

Disclosure of Potential Conflicts of Interest

M. Magnani is an employee of and holds ownership interest (including patents) in Diatheva SRL. D. Moricoli and V. Fiori are employees of Diatheva SRL. No potential conflicts of interest were disclosed by the other authors.

Authors' Contributions

Conception and design: K. Scotlandi, M. Magnani, C. Guerzoni
Development of methodology: V. Fiori, D. Moricoli, S. Dominici, C. Chiodoni, M. Magnani, K. Scotlandi, M.C. Manara, M. Terracciano, M. Pasello, M. Gellini
Acquisition of data (provided animals, acquired and managed patients, provided facilities, etc.): C. Guerzoni, M. Terracciano, M.C. Manara, M. Pasello, M. Sciandra, G. Nicoletti, C. Chiodoni, P.-L. Lollini, M.P. Colombo, P.M. Fornasari, P. Picci
Analysis and interpretation of data (e.g., statistical analysis, biostatistics, computational analysis): C. Guerzoni, M. Terracciano, M.C. Manara, M. Pasello, G. Nicoletti, M. Cianfriglia, K. Scotlandi
Writing, review, and/or revision of the manuscript: C. Guerzoni, V. Fiori, P.M. Fornasari, P.-L. Lollini, M.P. Colombo, P. Picci, M. Cianfriglia, M. Magnani, K. Scotlandi
Administrative, technical, or material support (i.e., reporting or organizing data, constructing databases): K. Scotlandi, M.C. Manara, M. Terracciano, M. Pasello, P.M. Fornasari, P. Picci, D. Moricoli, V. Fiori, M. Sciandra, S. Dominici, M. Gellini, C. Guerzoni
Study supervision: M. Magnani, K. Scotlandi
Other (engineering and expression of C7 diabody): V. Fiori, D. Moricoli, S. Dominici

Acknowledgments

The authors thank Ghislaine Bernard, INSERM U576, Faculté de Médicine, Nice, France, for kindly providing 0662-mAb hybridoma; Enrico Lucarelli (Rizzoli Institute) and Laura Bonsi (University of Bologna, Bologna, Italy) for sharing primary mesenchymal stem cell cultures; Michela Rugolo (University of Bologna, Bologna, Italy), Anna Maria Porcelli (University of Bologna, Bologna, Italy), and Fabiola Moretti (Cell Biology and Neurobiology Institute-CNR/Fondazione Santa Lucia) for their precious scientific advice and materials, and Cristina Ghinelli for help in editing the manuscript.

Grant Support

This work was supported by grants from the Italian Association for Cancer Research (IG2013_14049 to K. Scotlandi; and AIRC 14194 to M.P. Colombo), Liddy Shriver Foundation by the Italian Ministry of Research and Instruction, F.I.R.B. project number RBAP11884 M_005 (to K. Scotlandi), and Regione Emilia Romagna Project: POR-FESR2007-2013.

The costs of publication of this article were defrayed in part by the payment of page charges. This article must therefore be hereby marked *advertisement* in accordance with 18 U.S.C. Section 1734 solely to indicate this fact.

Received February 27, 2014; revised September 18, 2014; accepted October 12, 2014; published OnlineFirst December 11, 2014.

References

1. Womer RB, West DC, Krailo MD, Dickman PS, Pawel BR, Grier HE, et al. Randomized controlled trial of interval-compressed chemotherapy for the treatment of localized Ewing sarcoma: a report from the Children's Oncology Group. J Clin Oncol 2012;30:4148–54.
2. Longhi A, Ferrari S, Tamburini A, Luksch R, Fagioli F, Bacci G, et al. Late effects of chemotherapy and radiotherapy in osteosarcoma and Ewing sarcoma patients: the Italian Sarcoma Group Experience (1983–2006). Cancer 2012;118:5050–9.
3. Luksch R, Tienghi A, Hall KS, Fagioli F, Picci P, Barbieri E, et al. Primary metastatic Ewing's family tumors: results of the Italian Sarcoma Group and Scandinavian Sarcoma Group ISG/SSG IV Study including myeloablative chemotherapy and total-lung irradiation. Ann Oncol 2012;23:2970–6.
4. Scotlandi K, Baldini N, Cerisano V, Manara MC, Benini S, Serra M, et al. CD99 engagement: an effective therapeutic strategy for Ewing tumors. Cancer Res 2000;60:5134–42.
5. Scotlandi K, Perdichizzi S, Bernard G, Nicoletti G, Nanni P, Lollini PL, et al. Targeting CD99 in association with doxorubicin: an effective combined treatment for Ewing's sarcoma. Eur J Cancer 2006;42:91–6.
6. Goodfellow P, Banting G, Sheer D, Ropers HH, Caine A, Ferguson-Smith MA, et al. Genetic evidence that a Y-linked gene in man is homologous to a gene on the X chromosome. Nature 1983;302:346–9.
7. Choi EY, Park WS, Jung KC, Kim SH, Kim YY, Lee WJ, et al. Engagement of CD99 induces up-regulation of TCR and MHC class I and II molecules on the surface of human thymocytes. J Immunol 1998;161:749–54.
8. Kim MK, Choi YL, Kim SH, Choi EY, Park WS, Bae YM, et al. MHC class II engagement inhibits CD99-induced apoptosis and up-regulation of T cell receptor and MHC molecules in human thymocytes and T cell line. FEBS Lett 2003;546:379–84.

Published OnlineFirst December 11, 2014; DOI: 10.1158/1078-0432.CCR-14-0492

9. Bremond A, Meynet O, Mahiddine K, Coito S, Tichet M, Scotlandi K, et al. Regulation of HLA class I surface expression requires CD99 and p230/golgin-245 interaction. Blood 2009;113:347–57.
10. Yoon SS, Jung KI, Choi YL, Choi EY, Lee IS, Park SH, et al. Engagement of CD99 triggers the exocytic transport of ganglioside GM1 and the reorganization of actin cytoskeleton. FEBS Lett 2003;540:217–22.
11. Alberti I, Bernard G, Rouquette-Jazdanian AK, Pelassy C, Pourtein M, Aussel C, et al. CD99 isoforms expression dictates T cell functional outcomes. FASEB J 2002;16:1946–8.
12. Bixel MG, Petri B, Khandoga AG, Khandoga A, Wolburg-Buchholz K, Wolburg H, et al. A CD99-related antigen on endothelial cells mediates neutrophil but not lymphocyte extravasation in vivo. Blood 2007;109:5327–36.
13. Dworzak MN, Froschl G, Printz D, Zen LD, Gaipa G, Ratei R, et al. CD99 expression in T-lineage ALL: implications for flow cytometric detection of minimal residual disease. Leukemia 2004;18:703–8.
14. Pliyev BK, Shepelev AV, Ivanova AV. Role of the adhesion molecule CD99 605Q10 in platelet-neutrophil interactions. Eur J Haematol 2013; 91:456–61.
15. Llombart-Bosch A, Machado I, Navarro S, Bertoni F, Bacchini P, Alberghini M, et al. Histological heterogeneity of Ewing's sarcoma/PNET: an immunohistochemical analysis of 415 genetically confirmed cases with clinical support. Virchows Arch 2009;455:397–411.
16. Fisher C. Synovial sarcoma. Ann Diagn Pathol 1998;2:401–21.
17. Rajaram V, Brat DJ, Perry A. Anaplastic meningioma versus meningeal hemangiopericytoma: immunohistochemical and genetic markers. Hum Pathol 2004;35:1413–8.
18. Seol HJ, Chang JH, Yamamoto J, Romagnuolo R, Suh Y, Weeks A, et al. Overexpression of CD99 increases the migration and invasiveness of human malignant glioma cells. Genes Cancer 2012;3:535–49.
19. Lessnick SL, Ladanyi M. Molecular pathogenesis of Ewing sarcoma: new therapeutic and transcriptional targets. Annu Rev Pathol 2012;7:145–59.
20. Rocchi A, Manara MC, Sciandra M, Zambelli D, Nardi F, Nicoletti G, et al. CD99 inhibits neural differentiation of human Ewing sarcoma cells and thereby contributes to oncogenesis. J Clin Invest 2010;120:668–80.
21. Miyagawa Y, Okita H, Nakaijima H, Horiuchi Y, Sato B, Taguchi T, et al. Inducible expression of chimeric EWS/ETS proteins confers Ewing's family tumor-like phenotypes to human mesenchymal progenitor cells. Mol Cell Biol 2008;28:2125–37.
22. Hu-Lieskovan S, Zhang J, Wu L, Shimada H, Schofield DE, Triche TJ. EWS-FLI1 fusion protein up-regulates critical genes in neural crest development and is responsible for the observed phenotype of Ewing's family of tumors. Cancer Res 2005;65:4633–44.
23. Franzetti GA, Laud-Duval K, Bellanger D, Stern MH, Sastre-Garau X, Delattre O. MiR-30a-5p connects EWS-FLI1 and CD99, two major therapeutic targets in Ewing tumor. Oncogene 2013;32:3915–21.
24. Jung KC, Kim NH, Park WS, Park SH, Bae Y. The CD99 signal enhances Fas-mediated apoptosis in the human leukemic cell line, Jurkat. FEBS Lett 2003;554:478–84.
25. Cerisano V, Aalto Y, Perdichizzi S, Bernard G, Manara MC, Benini S, et al. Molecular mechanisms of CD99-induced caspase-independent cell death and cell-cell adhesion in Ewing's sarcoma cells: actin and zyxin as key intracellular mediators. Oncogene 2004;23:5664–74.
26. Gellini M, Ascione A, Flego M, Mallano A, Dupuis ML, Zamboni S, et al. Generation of human single-chain antibody to the 99 cell surface determinant specifically recognizing Ewing's sarcoma sumor cells. Curr Pharm Biotechnol 2012;14:449–63.
27. Holliger P, Hudson PJ. Engineered antibody fragments and the rise of single domains. Nat Biotechnol 2005;23:1126–36.
28. Sciandra M, Marino MT, Manara MC, Guerzoni C, Grano M, Oranger A, et al. CD99 drives terminal differentiation of osteosarcoma cells by acting as a spatial regulator of ERK 1/2. J Bone Miner Res 2014;29:1295–309.
29. Chou TC. Assessment of synergistic and antagonistic effects of chemotherapeutic agents in vitro. Contrib Gynecol Obstet 1994;19:91–107.
30. Bennett MR. Mechanisms of p53-induced apoptosis. Biochem Pharmacol 1999;58:1089–95.
31. Ottaviano L, Schaefer KL, Gajewski M, Huckenbeck W, Baldus S, Rogel U, et al. Molecular characterization of commonly used cell lines for bone tumor research: a trans-European EuroBoNet effort. Genes Chromosomes Cancer 2010;49:40–51.
32. Zhang W, Funk WD, Wright WE, Shay JW, Deisseroth AB. Novel DNA binding of p53 mutants and their role in transcriptional activation. Oncogene 1993;8:2555–9.
33. Chan KT, Lung ML. Mutant p53 expression enhances drug resistance in a hepatocellular carcinoma cell line. Cancer Chemother Pharmacol 2004;53:519–26.
34. Neilsen PM, Pishas KI, Callen DF, Thomas DM. Targeting the p53 Pathway in Ewing Sarcoma. Sarcoma 2011;2011:746939.
35. Kubbutat MH, Jones SN, Vousden KH. Regulation of p53 stability by Mdm2. Nature 1997;387:299–303.
36. Vassilev LT, Vu BT, Graves B, Carvajal D, Podlaski F, Filipovic Z, et al. In vivo activation of the p53 pathway by small-molecule antagonists of MDM2. Science 2004;303:844–8.
37. Gordon MD, Corless C, Renshaw AA, Beckstead J. CD99, keratin, and vimentin staining of sex cord-stromal tumors, normal ovary, and testis. Mod Pathol 1998;11:769–73.
38. Husak Z, Dworzak MN. CD99 ligation upregulates HSP70 on acute lymphoblastic leukemia cells and concomitantly increases NK cytotoxicity. Cell Death Dis 2012;3:e425.
39. Bernard G, Breittmayer JP, de Matteis M, Trampont P, Hofman P, Senik A, et al. Apoptosis of immature thymocytes mediated by E2/CD99. J Immunol 1997;158:2543–50.
40. Imbert AM, Belaaloui G, Bardin F, Tonnelle C, Lopez M, Chabannon C. CD99 expressed on human mobilized peripheral blood CD34+ cells is involved in transendothelial migration. Blood 2006;108:2578–86.
41. Amaral AT, Manara MC, Berghuis D, Ordoñez JL, Biscuola M, Lopez-García MA, et al. Characterization of human mesenchymal stemcells from Ewing sarcoma patients: pathogenetic implications. PLoS ONE 2014;9 e85814.
42. Wittel UA, Jain M, Goel A, Chauhan SC, Colcher D, Batra SK. The in vivo characteristics of genetically engineered divalent and tetravalent single-chain antibody constructs. Nucl Med Biol 2005;32:157–64.
43. Rudnick SI, Adams GP. Affinity and avidity in antibody-based tumor targeting. Cancer Biother Radiopharm 2009;24:155–61.
44. Husak Z, Printz D, Schumich A, Potschger U, Dworzak MN. Death induction by CD99 ligation in TEL/AML1-positive acute lymphoblastic leukemia and normal B cell precursors. J Leukoc Biol 2010;88:405–12.
45. Accardi L, Di Bonito P. Antibodies in single-chain format against tumour-associated antigens: present and future applications. Curr Med Chem 2010;17:1730–55.
46. Ladanyi M, Lewis R, Jhanwar SC, Gerald W, Huvos AG, Healey JH. MDM2 and CDK4 gene amplification in Ewing's sarcoma. J Pathol 1995;175:211–7.
47. Tacar O, Sriamornsak P, Dass CR. Doxorubicin: an update on anticancer molecular action, toxicity and novel drug delivery systems. J Pharm Pharmacol 2013;65:157–70.
48. Dworzak MN, Fritsch G, Buchinger P, Fleischer C, Printz D, Zellner A, et al. Flow cytometric assessment of human MIC2 expression in bone marrow, thymus, and peripheral blood. Blood 1994;83:415–25.
49. Stork R, Campigna E, Robert B, Muller D, Kontermann RE. Biodistribution of a bispecific single-chain diabody and its half-life extended derivatives. J Biol Chem 2009;284:25612–9.
50. Dotto GP. p21(WAF1/Cip1): more than a break to the cell cycle? Biochim Biophys Acta 2000;1471:M43–56.

Published OnlineFirst December 11, 2014; DOI: 10.1158/1078-0432.CCR-14-0492

Clinical Cancer Research

CD99 Triggering in Ewing Sarcoma Delivers a Lethal Signal through p53 Pathway Reactivation and Cooperates with Doxorubicin

Clara Guerzoni, Valentina Fiori, Mario Terracciano, et al.

Clin Cancer Res 2015;21:146-156. Published OnlineFirst December 11, 2014.